Experimental researches of magnetoreological elestomers stiffness changes under external magnetic field

Grzegorz Sławiński[1], Danuta Miedzińska[1], Tadeusz Niezgoda[1] and Anna Boczkowska[2]

[1]*Faculty of Mechanical Engineering, Military University of Technology*
Gen. Sylwestra Kaliskiego 2, 00-908 Warsaw, Poland
e-mail: gslawinski@wat.edu.pl

[2]*Faculty of Materials Science and Engineering, Warsaw University of Technology*
Wołoska 141, 02-507 Warsaw, Poland
e-mail: abocz@meil.pw.edu.pl

Abstract

Magnetorheological elastomers (MREs) belong to the group of so-called smart materials which respond to an external stimulus by changing their viscoelastic properties. Magnetorheological (MR) material can be fluid, gel or solid material like elastomer. The mechanical properties of the MR materials undergo a change when subjected to an external magnetic field. The MREs are interesting candidates for the active stiffness and vibration control of structural systems [1]. In the paper the experimental results of the dynamic and static tests of the MRE samples cured without and under magnetic field are presented and compared. The influence of the internal structure of the researched material on its strength behaviour is taken into consideration. The results of experimental tests carried out in order to determine the parameters necessary to build the numerical model were included in the paper.

Keywords: experimental mechanics, material properties, smart materials

1. Introduction

Magnetorheological elastomers (MREs) are materials with rheological properties which can be changed in a continuous way, rapidly and reversibly by the applied magnetic field. They can also change their shape and size. The increase in the material stiffness can reach even 60% of the initial value [2]. They are the solid analogues of magnetorheological fluids (MRFs), consisting of magnetically permeable particles (such as iron) added to a viscoelastic polymeric material prior to crosslinking. Before the curing process of the polymer, a strong external magnetic field is applied. The field induces dipole moments within the particles which seek minimum energy states. The chains of particles with collinear dipole moments are formed and cured of the polymeric matrix material which locks the chains in place. In this orientation, the particles can form separate chains in the three-dimensional simple lattice structures or even more complicated structures, where particles have multiple interaction points [3]. Process of forming chains in MREs was shown in the Fig. 1.

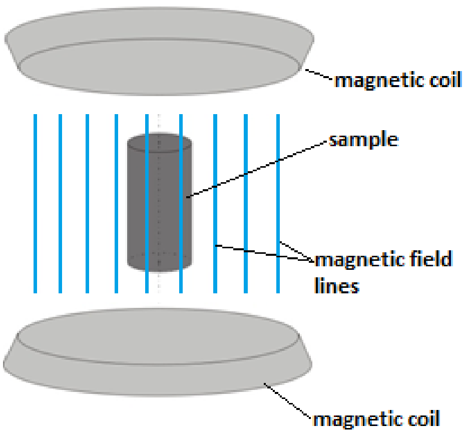

Figure 1: Schematic explanation of the manufacturing method

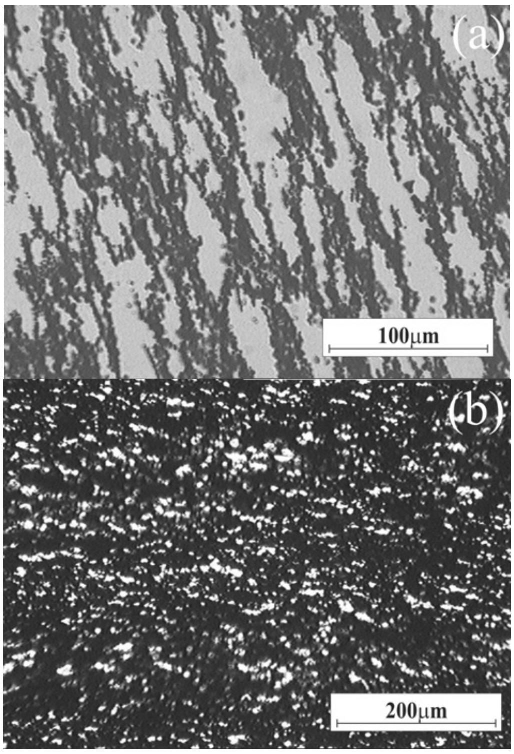

Figure 2: Microstructure of PU cured under magnetic field of 300 mT, filled with carbonyl-iron particles: (a) 11.5 vol%, (b) 33 vol% [4]

According to the previous tests and literature studies [5, 6, 7] the carbonyl-iron volume content in the matrix, lower than 33%, leads to the formation of well organized chains of particles.

Figure 2 presented the typical microstructure of the MRE cured under the magnetic field of 300mT, filled with carbonyl iron particles of 11,5 and 33vol%.

Applications of MR elastomers include automotive bushings and engine mounts, where significant changes in spring constant due to the applied magnetic field can be used to control stiffness and damping properties dynamically.

2. Experimental researches of MRE description

For the purposes of experimental researches the cylindrical samples of 55 mm diameter and 70 mm height were prepared. The samples were made of the polyurethane elastomer PU 70/30 with the admixture of the ferromagnetic particles.

The samples made of elastomer with the carbonyl iron particles volume fraction of 11.5% were analyzed. The samples with ferromagnetic particles were cured without as well as under the external, parallel to the vertical axis of the sample, magnetic field of the 300 mT intensity.

The researched specimens were as follows:

- 1WF - elastomer PU 70/30 with the carbonyl iron particles volume fraction of 11.5%, cured without the external magnetic field,
- 2WF - elastomer PU 70/30 with the carbonyl iron particles volume fraction of 11.5%, cured without the external magnetic field,
- 3F - elastomer PU 70/30 with the carbonyl iron particles volume fraction of 11.5%, cured under the external magnetic field,
- 4F - elastomer PU 70/30 with the carbonyl iron particles volume fraction of 11.5%, cured under the external magnetic field.

The experiments were carried out on the materials testing machine for static and dynamic loads INSTRON 8802 (see Fig. 3). The machine was additionally equipped with the measurement head of 4kN scope and the magnetic coil that produces the magnetic field of the intensity up to 500 mT.

Figure 3: Research equipment

Both static and dynamic (cycled) load was applied to the MRE samples. The shapes of the load curves for each type of the testing machine kinematic constraint were presented in Fig. 4. In the case of the static tests, the load was linear and in the case of the dynamic tests the sinusoid cyclic variable load was used. During the dynamics tests the temperature of the samples can rise. In case of MREs it may influence on its material properties. To avoid the influence of temperature the frequency in the test in case of elastomers used should not be more than 5 Hz. The applied load frequency was 1 Hz in each presented test. The samples were cyclically compressed of the 10, 15, 20 and 25 % of their height. Both static and dynamic tests were carried out under the magnetic field of the 300 mT intensity.

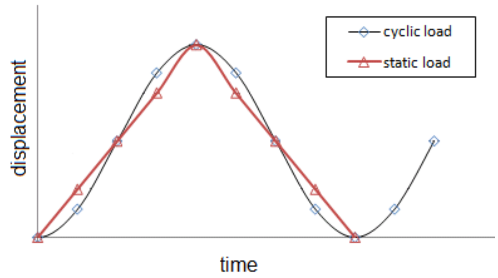

Figure 4: Shapes of load curves

3. Experimental results

During the experiments the continuous measurement of the testing machine clamps load and displacement was led. During the static tests the measurements were registered for the compression and unloading phase. During the dynamic cyclic tests the steering equipment readings were continuously observed and simultaneously the parameters of the registered cycle were saved. The exemplary results for the samples compressed of the 25 % of their height were shown in Fig. 5 to 8.

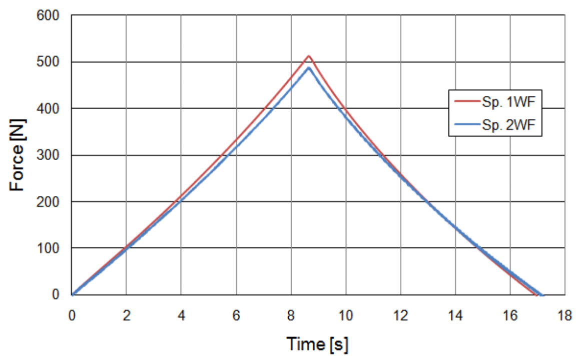

Figure 5: Results of the static tests for MRE samples cured without the external magnetic field

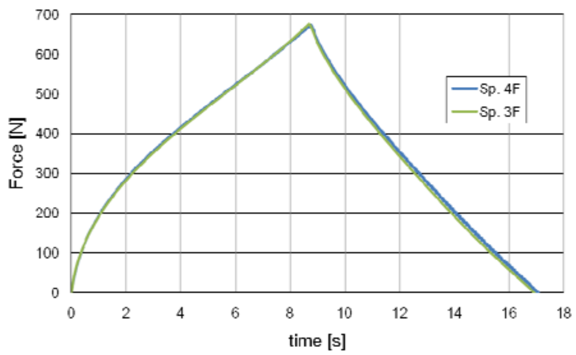

Figure 6: Results of the static tests for MRE samples cured under the external magnetic field

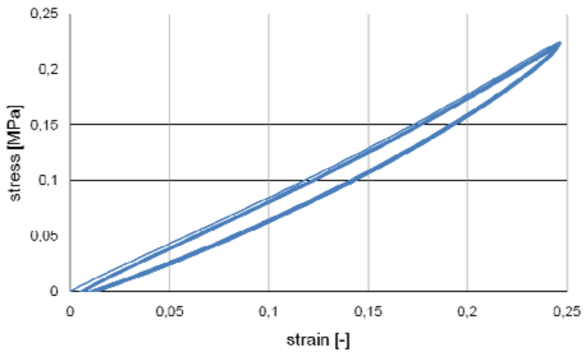

Figure 7: Results of the dynamic tests for MRE samples cured without the external magnetic field

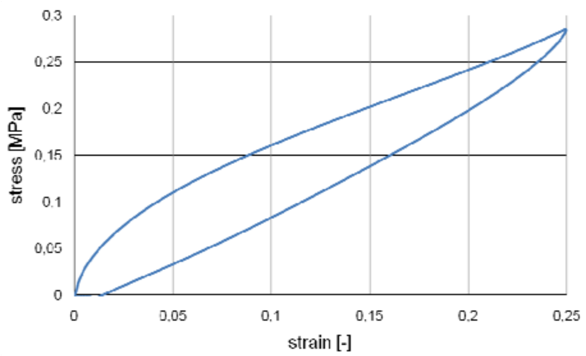

Figure 8: Results of the static tests for MRE samples cured under the external magnetic field

The visualization of the static tests results for samples 1WF and 3F was shown in Fig. 9. Fig. 10 presents the hysteresis loops in the load – displacement charts that were observed during the dynamic tests (samples 2FW and 4F).

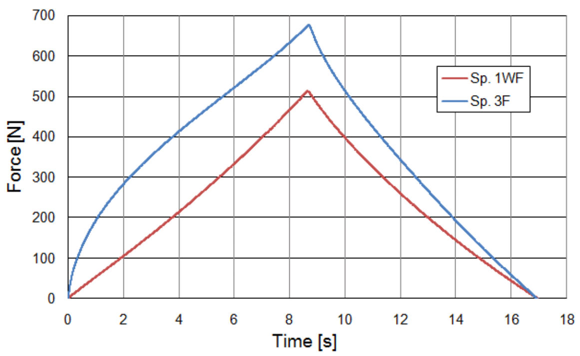

Figure 9: Results of the static tests for MRE samples 1WF and 3F

On the base of the obtained results the force maximum values in each dynamic and static test were calculated. Those values were presented in Table 1. It can be concluded that the results from the tests for the samples cured under the magnetic field are about 30 % higher than the results from the tests for the samples cured without the magnetic field.

In addition, the dumping coefficient (the energy dissipation coefficient) was calculated with the use of Equation 1 [8]:

$$\psi = \frac{w_2}{w_1} = \frac{L_{ob} - L_{od}}{L_{ob}} \tag{1}$$

where: w_2 – dissipation energy in one cycle, w_1- elastic strain energy. The coefficient values were shown in Table 1.

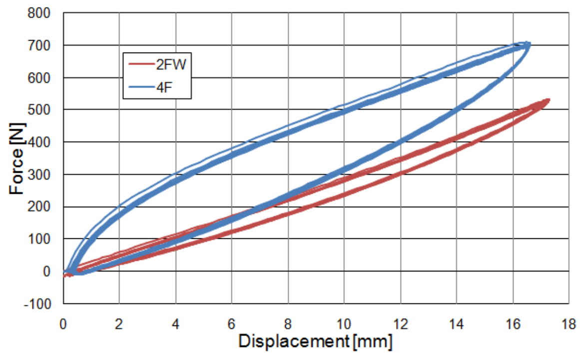

Figure 10: Results of the dynamic tests for MRE samples 2WF and 4F

4. Macrostructural numerical analyses

The Mooney – Rivlin material model [5] was applied to the numerical analysis of the hyperelastic behaviour of the elastomer. In that model the strain energy density function W is a linear combination of two invariants of the left Cauchy-Green deformation tensor [6]. This function can be assumed as:

$$W = \sum_{i+j=1}^{n} C_{ij} (I_1 - 3)^i (I_2 - 3)^j \tag{2}$$

where C_{ij} are empirically determined material constants, I_1 and I_2 are the first and the second invariants of the deviatoric component of the left Cauchy-Green deformation tensor described as follows:

$$I_1 = \lambda_1^2 + \lambda_2^2 + \lambda_3^2 \tag{3a}$$

$$I_2 = \lambda_1^2 \lambda_2^2 + \lambda_2^2 \lambda_3^2 + \lambda_3^2 \lambda_1^2 \tag{3b}$$

where λ_1, λ_2, λ_3 are the elongations of the element in directions shown in Fig. 11.

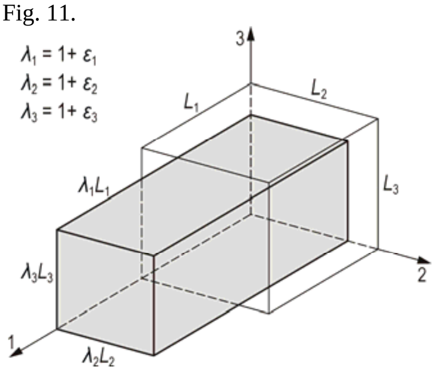

Figure 11: Elongations of the element for the Mooney-Rivlin material model

The numerical model, shown in Fig. 12, was developed with the use of solid elements Hex8 [9]. A static numerical analysis was carried out with the use of MSC Marc computer code. This software enables carrying out analyses taking into account large displacements and deformations. Moreover, it includes a module for modelling highly elastic materials, such as rubber, elastomers and others. Compression was performed with two rigid plates – a stationary and a moving one (displacement of 25% sample height). The parameters for the Mooney-Rivlin material model were calculated with the use of MSC Mentat application and are presented in Table 1.

Table 1: Experimental and numerical results

	Force [N]		Dumping coefficient		Mooney-Rivlin constants	
	Static	Dynamic	Static	Dynamic	C_{10}	C_{01}
Sp. 1WF	512.87	528.06	0.1003	0.1620	0.121804	0
Sp. 2WF	487.35	505.12	0.0722	0.1569	0.123209	0
Sp. 3F	676.32	702.54	0.3319	0.3795	0	0.261841
Sp. 4F	675.14	708.74	0.3279	0.3677	0	0270912

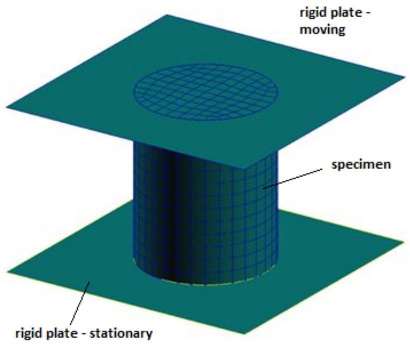

Fig. 12. FE model of elastomer sample

The results of the numerical analysis with the comparison to the experiment are presented in Fig. 13. The very high correspondence between experimental and numerical analyses is visible clearly.

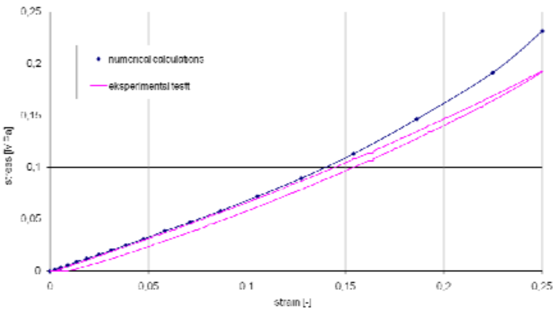

Fig. 13. Numerical calculations and experimental results for pure elastomer

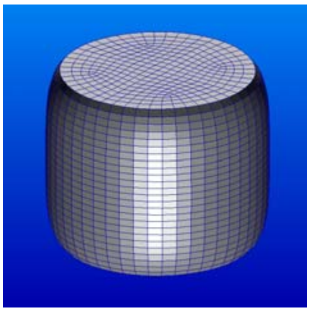

Fig. 14. FE analysis of MRE – deformations

Deformations of specimen during static load were presented in Fig. 14. In this case also the very high correspondence between experimental and numerical analyses is clearly visible.

Figure 15 presents change of dumping coefficient for few levels of the compression. For specimens cured without the external magnetic field the dumping coefficient has a constant value. In case of specimens cured under the external magnetic field value of the dumping coefficient decreases with the rising of compression.

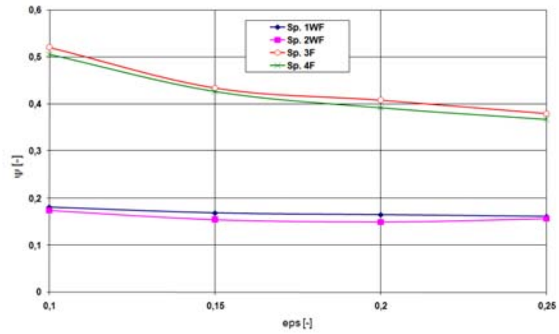

Fig. 14. Change of dumping coefficient

5. Summary

The experimental results of the dynamic and static tests of the MRE samples cured without and under magnetic field were presented and compared in the paper. The influence of the MRE internal structure and external magnetic field on the researched strength parameters was strictly proofed.

References

[1] Kallio, M., The elastic and damping properties of magnetorheological elastomers, University of Tampere, 2005

[2] Miedzinska, D., Boczkowska, A., Zubko, K., Numerical verification of three point bending experiment of magnetorheological elastomer (MRE) in magnetic field, Journal of Physics: Conference Series 240 (2010) 012158.

[3] Boczkowska, A., Awietjan, S., Urethane Magnetorheological Elastomers – Manufacturing, Microstructure and Properties, Solid State Phenomena, Volume 154, pp. 107-112, 2009.

[4] Boczkowska A., Awietjan S. F., Wroblewski R., Microstructure–property relationships of urethane magnetorheological elastomers, Smart Mater. Struct. 16 ,1924–1930, 2007

[5] Coquelle E., Properietes elastiques et viscoelastiques de materiaux composities adaptatifs. Du traitement de surface des charges au comportement magnetorheologique. PHD thesis, Universite de Nice Sophia-Antipolis, 2005.

[6] Bossis G., Lacis S., Meunier A., Volkova O., Magnetorheological fluids, Journal of Magnetism and Magnetic Materials 252 (2002) 224-228

[7] Shen Y., MGolnaraghi.F., Heppler G.R., Experimental Research and Modeling of Magnethoreological Elastomers, Journal of Intelligent Material Systems and Structures, 15 (2004) 27-35

[8] Polish Standard PN 78/C-01604

[9] Marc 2007 r1 User Guide.